Kinematic Controllability for Decoupled Trajectory Planning in Underactuated Mechanical Systems

Francesco Bullo, *Member IEEE*, and Kevin M. Lynch, *Member IEEE*

Abstract— **We introduce the notion of *kinematic controllability* for second-order underactuated mechanical systems. For systems satisfying this property, the problem of planning fast collision-free trajectories between zero velocity states can be decoupled into the computationally simpler problems of path planning for a kinematic system followed by time-optimal time scaling. While this approach is well known for fully actuated systems, until now there has been no way to apply it to underactuated dynamic systems. The results in this paper form the basis for efficient collision-free trajectory planning for a class of underactuated mechanical systems including manipulators and vehicles in space and underwater environments.**

Keywords— **trajectory planning, underactuated manipulation, nonlinear controllability, affine connections**

I. Introduction

The problem of finding the time-optimal trajectory for a fully actuated robot manipulator along a specified path is a classical one in robotics. This problem has been solved by algorithms proposed by Bobrow *et al.* [1] and Shin and McKay [2], and later enhancements due to Pfeiffer and Johanni [3], Slotine and Yang [4], and Shiller and Lu [5]. These algorithms find the minimum-time time scaling of the path which respects the actuator constraints.

With the time-scaling algorithms in hand, the problem of finding a fast collision-free trajectory for an n joint manipulator in its $2n$-dimensional state space can be decoupled into the computationally simpler problems of planning paths in the n-dimensional configuration space (considering joint limits and obstacles) followed by time-optimal time scaling according to the manipulator dynamics. Any complex geometric configuration constraints are dealt with in the first phase, irrespective of the robot dynamics. Shiller and Dubowsky [6] use this decoupling to find globally near-time-optimal trajectories for a manipulator by considering the time-optimal time scaling of a large set of candidate paths. The efficiency of the search is enhanced by pruning candidate paths based on lower-bound estimates of the travel time, and trajectories are further optimized by local path optimization in addition to optimal time-scaling.

Unfortunately, the decoupled approach to trajectory planning does not extend in general to underactuated dynamic systems (second-order systems with fewer actuators than degrees-of-freedom). If the system has n degrees-of-freedom and m actuators ($m < n$), there are $n - m$ state-dependent equality constraints on the feasible accelerations of the system, which are sometimes referred to as second-order nonholonomic constraints. Examples of such systems include robot manipulators with passive joints, spacecraft, and underwater vehicles (ignoring drag). Since the acceleration constraints cannot be expressed as constraints on tangent vectors on the configuration space, meaningful path planning on the configuration space is precluded. In general, paths returned by a path planner will either be (1) infeasible for the robot, due to constraints arising from underactuation, or (2) feasible at only a certain speed.

In this paper we define a class of *kinematically controllable* underactuated systems for which it is possible to decouple trajectory planning between zero velocity states. The path planner uses a set of *decoupling velocity vector fields* defined on the configuration space to find paths which can be time scaled without violating the underactuation constraints. As a result, for this class of underactuated dynamic systems, we have the basis for efficient collision-free trajectory planning. This basic approach was first introduced in deriving a trajectory planner for a three degree-of-freedom robot with a passive third joint (Lynch *et al.* [7], [8]).

We envision pairing the decoupling ideas in this paper with planners for driftless nonholonomic systems. Examples include path planners for car-like mobile robots [9], [10]. An alternative to decoupled trajectory planning is trajectory planning directly in the $2n$-dimensional system state space. This is often referred to as *kinodynamic* planning. Complexity results and kinodynamic motion planners for a variety of fully actuated systems can be found in [11], [12], [13], [14], [15], [16]. To decrease the computational cost of kinodynamic motion planning, randomized approaches have been proposed by LaValle and Kuffner [17], [18] and Hsu *et al.* [19]. These algorithms compute search trees exploiting randomization and heuristics to speed up the exploration, and they have been applied to models of underactuated systems.

Our approach to reducing the computational complexity of trajectory planning for underactuated mechanical systems is based on using the structure of the system dynamics to naturally decouple the problem into path planning followed by time scaling.

Submitted as Regular Paper on November 2000, revised on May 2001 A short version of this work appeared in the Proceedings of the IEEE International Conference in Robotics & Automation, Seoul, Korea, April 2001.

Francesco Bullo is with the Coordinated Science Laboratory and the General Engineering Department at the University of Illinois at Urbana-Champaign, 1308 W Main St, Urbana, IL 61801, Tel: (217) 333-0656, Fax: (217) 244-1653, Email: `bullo@uiuc.edu`.

Kevin M. Lynch is with the Mechanical Engineering Department at Northwestern University, Evanston, IL 60208, Tel: (847) 467-5451, Fax: (847) 491-3915, Email: `kmlynch@northwestern.edu`

A. Brief overview of decoupled trajectory planning

Consider an underactuated second-order system of the form

$$M(q)\ddot{q} + C(q,\dot{q})\dot{q} + G(q) = \begin{bmatrix}\tau \\ 0\end{bmatrix},$$

where $q \in Q = \mathbb{R}^n$ is the configuration, $\tau \in \mathbb{R}^m$ is the control, and there are $n-m$ second-order constraints due to underactuation. Although we will consider more general models of underactuated mechanical systems, this is the form most often seen for underactuated manipulators, and it provides a connection to previous work on time-scaling paths for robotic manipulators.

Consider a path of the system $q(s)$ parameterized by $s \in [0,1]$ and a time scaling $s(t)$ which assigns a point on the path for each $t \in [0,T]$. $s(t)$ is twice-differentiable and $\dot{s}(t) > 0$ for all $t \in (0,T)$. (Such a time scaling is the output of the minimum-time algorithms described above.) Then the trajectory of the system can be written $q(s(t))$, and each of the $n-m$ constraints has the form

$$a(s)\ddot{s} + b(s)\dot{s}^2 + c(s) = 0, \tag{1}$$

where a, b, and c are inertial, centrifugal and Coriolis, and gravity terms, respectively, of the system in the constrained directions when restricted to the path. The path $q(s)$ is a *kinematic motion* if the constraints are satisfied for any time scaling, i.e., $\dot{s}, \ddot{s}$ arbitrary. A velocity vector field V is a *decoupling vector field* if all paths $q(s)$ satisfying

$$\frac{dq(s)}{ds} = V\left(q(s)\right)$$

are kinematic motions. The system is *locally kinematically controllable* if there exist p decoupling vector fields such that the kinematic system

$$\begin{aligned} \dot{q} &= \sum_{c=1}^{p} V_c(q) w_c \qquad (2)\\ (w_1,\ldots,w_p) &\in \{(\pm 1,0,\ldots,0),(0,\pm 1,0,\ldots,0),\ldots,\\ &\quad (0,\ldots,0,\pm 1)\} \end{aligned}$$

is locally controllable.

It is clear that a path $q(s)$ is a kinematic motion (satisfies the constraints (1)) if and only if $a(s) = b(s) = c(s) = 0$. The requirement that $c(s) = 0$ implies that the potential term is zero in the constrained directions. In this paper we satisfy this condition trivially by only considering systems with no potential terms.

Our focus is on efficient trajectory planning between zero velocity states. If the system is locally kinematically controllable, then there exists a feasible path between any two zero velocity states in the same open connected component of free configuration space, and we can apply any collision-free path planner for the driftless kinematic system (2); see for example [9], [10]. Because each segment of the resulting path follows one of the decoupling vector fields, the speed along the segment is limited only by actuator saturation limits, not by the underactuation constraints. Switches between decoupling vector fields must occur at zero velocity, so it is appropriate for the path planner to minimize the number of switches. An interesting open problem is the design of motion planners to minimize the number of switches for general driftless kinematic systems of the form (2).

B. Statement of contributions and organization

In this paper we formalize the notions of "decoupling vector field" and "kinematic controllability" in the coordinate-free setting of connections (see for example the work on configuration controllability by Lewis and Murray [20], and on motion planning via oscillatory controls by Bullo *et al.* [21]). We provide necessary and sufficient conditions for a vector field to be decoupling, and sufficient conditions for a system to be kinematically controllable.

Although finding decoupling vector fields is in general a difficult problem, it is possible to find a variety of example systems which are kinematically controllable. We first study in detail a planar three link manipulator with three revolute joints (the SCARA configuration or 3R) with a single unactuated joint. For all three actuator configurations we are able to find decoupling vector fields yielding kinematic controllability. We then demonstrate kinematic controllability for some vehicle models in space and underwater environments. Finally, we illustrate the application of kinematic controllability to decoupled trajectory planning with the example of a three-dimensional spacecraft. Trajectory planning is reduced to path planning via simple inverse kinematics, followed by time-scaling.

Section II gives a coordinate-free description of underactuated second-order mechanical systems. Section III provides tests for decoupling vector fields and kinematic controllability. Section IV gives a short catalog of kinematically controllable systems, presents a detailed study of planar three link manipulators, and presents results and examples for vehicles with symmetry. Section V gives an example of trajectory planning for a kinematically controllable system, and Section VI outlines some directions for future research.

II. Models of mechanical systems

We consider mechanical control systems with total energy equal to kinetic energy and control inputs bounded in magnitude. Examples include robot manipulators and vehicles.

Let $q = (q^1,\ldots,q^n) \in Q = \mathbb{R}^n$ be the configuration of the mechanical system, and M be the inertia tensor defining the kinetic energy and an inner product between vector fields on Q. In the coordinate system $(q^1,\ldots,q^n)$, M_{ij} denotes the (i,j) component of the square matrix M, and M^{ij} denotes the (i,j) component of the inverse matrix M^{-1}. Consider the control system:

$$\begin{gathered} \ddot{q}^i + \Gamma^i_{jk}(q)\dot{q}^j\dot{q}^k = Y^i_1(q)u_1 + \ldots + Y^i_m(q)u_m \qquad (3)\\ q(0) = q_0,\ \ \dot{q}(0) = 0, \end{gathered}$$

where the summation convention is in place for the indices j,k that run from 1 to n, and where:

(i) the n^3 scalar functions $\{q \mapsto \Gamma^i_{jk}(q) : i,j,k = 1,\dots,n\}$ are called Christoffel symbols[1] and are computed according to

$$\Gamma^k_{ij} = \frac{1}{2} M^{\ell k}\left(\frac{\partial M_{\ell j}}{\partial q^i} + \frac{\partial M_{\ell i}}{\partial q^j} - \frac{\partial M_{ij}}{\partial q^\ell}\right), \qquad (4)$$

(ii) $\{F_a : a = 1,\dots,m\}$ are the m input co-vector fields, and $\{Y_a = M^{-1}F_a : a = 1,\dots,m\}$ are the m input vector fields, and
(iii) the control inputs $(u_1,\dots,u_m)$ take values in the set $\mathcal{U}(q,\dot q) \subset \mathbb{R}^m$, where $\mathcal{U}(q,0)$ contains the origin of $\mathbb{R}^m$ in its interior for all $q \in \mathbb{R}^n$. An example of such a set is $\mathcal{U} = \{(u_1,\dots,u_m) |\ |u_i| \le 1\}$.

Systems endowed with fewer control actuators m than degrees of freedom n are called *underactuated*. Assuming the vector fields $Y_1,\dots,Y_m$ span the first m directions, the $n-m$ second-order constraints in system (3) read

$$\ddot q^i + \Gamma^i_{jk}(q)\dot q^j \dot q^k = 0, \quad i = m+1,\dots,n. \qquad (5)$$

A. Coordinate-free modeling

In a coordinate-free language, vector fields are written in terms of the canonical base $(\frac{\partial}{\partial q^1},\dots,\frac{\partial}{\partial q^n})$, and co-vector fields in terms of $(dq^1,\dots,dq^n)$. We will write both vectors and co-vectors fields as column vectors; given a co-vector field F and two vector fields X_1, X_2, two well defined operations are:

$$\langle F, X_1\rangle = F^T X_1$$
$$\langle\!\langle X_1\,,\, X_2\rangle\!\rangle = X_1^T M X_2.$$

Given two vector fields X, Y, the *covariant derivative* of Y with respect to X is the vector field $\nabla_X Y$ defined via

$$(\nabla_X Y)^i = \frac{\partial Y^i}{\partial q^j} X^j + \Gamma^i_{jk} X^j Y^k. \qquad (6)$$

This operation enjoys the property that

$$\nabla_{h_1 X_1}(h_2 X_2) = h_1 h_2 (\nabla_{X_1} X_2) + h_1 (\mathcal{L}_{X_1} h_2) X_2, \qquad (7)$$

where X_1, X_2 are vector fields, h_1, h_2 are scalar functions, and $\mathcal{L}_{X_1} h_2$ is the Lie derivative of h_2 along X_1. The operator ∇ is called the *Levi-Civita* connection for the mechanical system in equation (3); we refer to [22] for a more complete treatment. Using these concepts, the equations of motion can be rewritten as

$$\nabla_{\dot q}\dot q = \sum_{a=1}^m Y_a(q) u_a(t). \qquad (8)$$

Equation (8) is a coordinate-free version of equation (3).

Next, consider the $(m < n)$-dimensional co-distribution generated by the input co-vector fields $\mathrm{span}\{F_1,\dots,F_m\}$. Its annihilator is an $(n-m)$-dimensional distribution, which we shall call the *control annihilator distribution*, generated by vector fields $\{X_1,\dots,X_{n-m}\}$, such that

$$\langle F_a(q), X_b(q)\rangle = 0$$

for all $q \in \mathbb{R}^n$, $1 \le a \le m$, and $1 \le b \le n-m$. The vector fields X_b are easy to compute since they do not depend on the inertia tensor M. Given these vector fields, we compute

$$0 = \sum_{a=1}^m u_a \langle F_a, X_b\rangle = \langle M\nabla_{\dot q}\dot q, X_b\rangle = \langle\!\langle \nabla_{\dot q}\dot q\,,\, X_b\rangle\!\rangle.$$

Therefore, a curve $q(t)$ is a solution to the underactuated system in equation (3) only if it satisfies the $n-m$ constraints

$$\langle\!\langle \nabla_{\dot q}\dot q\,,\, X_b\rangle\!\rangle = 0. \qquad (9)$$

Equation (9) is a coordinate-free version of the second-order constraint in equation (5).

Example II.1 (A planar body with torque and force) Consider a planar body endowed with a control torque and a body-fixed control force applied through the center of mass. The configuration is $(x, y, \theta) \in \mathbb{R}^2 \times \mathbb{S}^1$, the kinetic energy is $\frac{1}{2}m(\dot x^2 + \dot y^2) + \frac{1}{2}I\dot\theta^2$, and the Christoffel symbols $\{\Gamma^k_{ij}, i,j,k = 1,2,3\}$ all vanish. The input co-vectors are $F_1 = d\theta$ and $F_2 = (\cos\theta)dx + (\sin\theta)dy$, and equation (8) reads

$$\ddot x = u_2\cos\theta, \quad \ddot y = u_2\sin\theta, \quad \ddot\theta = u_1.$$

The annihilator vector field is

$$X = (\sin\theta)\frac{\partial}{\partial x} - (\cos\theta)\frac{\partial}{\partial y}$$

and equation (9) reads

$$\ddot x\sin\theta - \ddot y\cos\theta = 0.$$

B. Computational issues

Given an arbitrary robot manipulator, it is often cumbersome to compute its Christoffel symbols, the inverse of its inertia matrix, and the covariant derivative of various relevant vector fields. This is true even for low-dimensional systems, such as the three degree-of-freedom manipulator described later in the paper. Accordingly, these computations are conveniently implemented in a Mathematica™ library. The library `MechSys` is presented in Appendix B.

III. Decoupling vector fields and kinematic controllability

The solution to the equations of motion for a mechanical system obeys the second-order differential equation (3) on the n-dimensional configuration space $Q = \mathbb{R}^n$. Alternatively, the system can be written as a first-order differential equation on the $2n$-dimensional tangent bundle $TQ = \mathbb{R}^{2n}$.

For mechanical control systems, we introduce the notion of *first-order* solutions described by vector fields on the configuration space Q. We require the solution to start and stop at rest.

[1] The functions $\{\Gamma^i_{jk}(q) : i,j,k = 1,\dots,n\}$ as defined in equation (4) are called Christoffel symbols in [22], [23]; in other references the $M^{\ell k}$ term is omitted [24].

Let $s : [0,T] \mapsto [0,1]$ be a twice-differentiable function such that $s(0) = 0, s(T) = 1, \dot{s}(0) = \dot{s}(T) = 0$, and $\dot{s}(t) > 0$ for all $t \in (0,T)$. We call a curve s with these properties a *time scaling*.

Definition III.1 (Decoupling vector field) The vector field V is a *decoupling vector field* for the mechanical system (3) if, for any time scaling s and for any initial condition q_0, the curve $q : [0,T] \mapsto Q$ solving

$$\dot{q}(t) = \dot{s}(t)V(q(t)), \qquad q(0) = q_0, \tag{10}$$

satisfies the $n-m$ constraints in equation (9).
We call such a curve $t \mapsto q(t)$ a *kinematic motion*.

Necessary and sufficient conditions for a decoupling vector field are as follows.

Lemma III.2: A vector field V is decoupling for the mechanical system (3) if and only if

$$\langle\langle V \, , \, X_b \rangle\rangle = 0 \tag{11}$$
$$\langle\langle \nabla_V V \, , \, X_b \rangle\rangle = 0 \tag{12}$$

for all $1 \leq b \leq n-m$.

Proof: Consider a curve $q : [0,T] \mapsto Q$ solving equation (10). We compute the quantity $\nabla_{\dot{q}}\dot{q}$ at $\dot{q} = \dot{s}V$ as

$$\begin{aligned} \nabla_{\dot{q}}\dot{q} &= \ddot{s}V + \dot{s}\nabla_{\dot{q}}V \\ &= \ddot{s}V + \dot{s}^2\nabla_V V, \end{aligned}$$

where we used the identity (7) and its extension to the setting of vector fields defined along curves; see [22]. Next, we recall that the curve $q : [0,T] \mapsto Q$ is a kinematic motion and V is a decoupling vector field if, for all time scalings s, the constraints (9) are satisfied. These equalities can be written as

$$0 = \langle\langle \left(\ddot{s}V + \dot{s}^2\nabla_V V\right) \, , \, X_b \rangle\rangle$$

for all $1 \leq b \leq n-m$. Since s is an arbitrary time scaling and q_0 is an arbitrary point, V and $\nabla_V V$ must separately have a vanishing inner product with X_b everywhere in Q. The same argument also shows the other implication. ∎

Roughly speaking, equation (12) encodes the requirement that motion along V at constant speed be feasible. Equation (11) requires the system to be able to speed up and slow down the motion along V. The terms $\langle\langle V \, , \, X_b \rangle\rangle$ and $\langle\langle \nabla_V V \, , \, X_b \rangle\rangle$ play the equivalent role of the coefficients $a(s)$ and $b(s)$ in equation (1), respectively.

Note that scalar multiples of decoupling vector fields are again decoupling, but linear combinations may not be decoupling. There are mechanical control systems for which no decoupling vector fields can be found; e.g., any mechanical system with a single control vector field Y such that $\nabla_Y Y \notin \text{span}\{Y\}$. The maximum number of linearly independent decoupling vector fields is m.

As described in the introduction, decoupling vector fields reduce the complexity of motion planning problems by turning a dynamic problem into a driftless kinematic one. Accordingly, it is of interest to define the class of systems for which this approach applies.

Definition III.3 (Kinematic controllability) The mechanical system (3) is *kinematically controllable* if every point in the configuration space Q is reachable via a sequence of kinematic motions. The system (3) is *locally kinematically controllable* if for any $q \in Q$ and any neighborhood U_q of q, the set of reachable configurations from q by kinematic motions remaining in U_q contains q in its interior.

Obviously, the main difficulty is that there might not be enough decoupling fields for controllability. A sufficient test for local kinematic controllability is given below. We assume the reader to be familiar with the notions of involutive closure and the Lie algebra rank condition for local controllability; see [24].

Lemma III.4: The system (3) is locally kinematically controllable if there exist $p \leq m$ vector fields $V_1, \ldots, V_p$ such that
(i) $0 = \langle\langle X_b \, , \, V_c \rangle\rangle = \langle\langle X_b \, , \, \nabla_{V_c} V_c \rangle\rangle$ for all $1 \leq b \leq n-m$ and $1 \leq c \leq p$, and
(ii) the involutive closure of $\{V_1, \ldots, V_p\}$ has rank n at all $q \in \mathbb{R}^n$.

Proof: Property *(i)* ensures that the vector fields V_c are decoupling. Property *(ii)* ensures the local controllability of the driftless kinematic system (2)

$$\begin{aligned} \dot{q} &= \sum_{c=1}^{p} V_c(q)w_c \\ (w_1, \ldots, w_p) &\in \{(\pm 1, 0, \ldots, 0), (0, \pm 1, 0, \ldots, 0), \ldots, \\ &\quad (0, \ldots, 0, \pm 1)\} \end{aligned}$$

and therefore every point in the configuration space is reachable. In the presence of obstacles, a collision-free path exists between any two points in an open connected set of the configuration space. ∎

Finally, we compare our novel characterization of controllability with the notions of small-time local controllability (STLC) and of small-time local configuration controllability (STLCC); see [25], [20]. It is interesting to do so since the three notions refer to the system and initial conditions in equation (3). Local kinematic controllability implies STLCC, while the opposite is not true. In other words, local kinematic controllability is only one way in which a mechanical system can be STLCC. Local kinematic controllability is neither implied by, nor implies, STLC.

Example III.5 (A planar body with torque and force) We continue to analyze the planar body in Example II.1. As decoupling vector fields we propose pure rotation and translation along the line of force:

$$\begin{aligned} V_1 &= Y_1 = M^{-1}F_1 = \frac{1}{I}\frac{\partial}{\partial\theta} \\ V_2 &= Y_2 = M^{-1}F_2 = \frac{1}{m}(\cos\theta)\frac{\partial}{\partial x} + \frac{1}{m}(\sin\theta)\frac{\partial}{\partial y}. \end{aligned}$$

By construction we have $\langle\langle V_1 \, , \, X \rangle\rangle = \langle\langle V_2 \, , \, X \rangle\rangle = 0$. Furthermore, an application of equation (6) provides:

$$\begin{aligned} \nabla_{V_1}V_1 &= \frac{1}{I^2}\nabla_{\frac{\partial}{\partial\theta}}\frac{\partial}{\partial\theta} = 0 \\ \nabla_{V_2}V_2 &= \frac{1}{m^2}\nabla_{\left(\cos\theta\frac{\partial}{\partial x} + \sin\theta\frac{\partial}{\partial y}\right)}\left(\cos\theta\frac{\partial}{\partial x} + \sin\theta\frac{\partial}{\partial y}\right) = 0. \end{aligned}$$

In summary, V_1, V_2 are decoupling vector fields, and since $\{V_1, V_2, [V_1, V_2]\}$ is full rank, the system is locally kinematically controllable.

A. Computing decoupling vector fields

Motivated by the sufficient test for local kinematic controllability in Lemma III.4, we investigate how to find decoupling vector fields V. It is sometimes possible to design educated guesses on possible decoupling vector fields by relying on intuition about the system's behavior. One instance is given by the steady translation and pure rotation vector fields defined in Example III.5. As a first step in the study of more complicated systems, one can start by defining similar vector fields with a clear physical meaning. A second set of useful concepts comes from the theory of Lagrangian reduction and of conservation laws. These ideas are relevant whenever the system's kinetic energy is invariant under a group action, typically a rigid body displacement. In such cases, one should look for decoupling fields which are themselves invariant under the group action.

Although these ideas are helpful, a direct algorithm would simplify the task. According to Lemma III.2, two conditions need to be satisfied. To automatically satisfy the first one while losing no generality, we write

$$V(q) = \sum_{a=1}^{m} h^a(q) Y_a(q),$$

where $h^1, \ldots, h^m$ are arbitrary scalar functions on Q. According to equation (7), we compute

$$\nabla_V V = \sum_{a=1}^{m} \sum_{b=1}^{m} \Big(h^a h^b \nabla_{Y_a} Y_b + h^a \left(\mathcal{L}_{Y_a} h^b \right) Y_b \Big),$$

so that the vector field V is decoupling if

$$0 = \sum_{a=1}^{m} \sum_{b=1}^{m} h^a(q) h^b(q) \, \langle\langle X_c \, , \, \nabla_{Y_a} Y_b \rangle\rangle(q) \qquad (13)$$

for all $q \in Q$, and for all $1 \leq c \leq n - m$. Equation (13) is quadratic in the unknown functions $h^1, \ldots, h^m$ and configuration dependent. Although no general solution methodology appears to be available, solutions can be found on a case by case basis. For example, in any three degrees-of-freedom system with two control inputs, only one quadratic equation needs to be solved as a function of two unknown variables. This latter problem is tractable with the aid of symbolic manipulation software.

IV. Examples and extensions

Numerous systems fit the requirements of Lemma III.4, allowing the decoupling of trajectory planning. Examples include:
(i) All systems subject to nonholonomic or conservation law constraints for which kinematic equations of motion can be written. These systems are described for example in [26] as "driftless locomotion systems" and in [27] as "kinematic mechanical systems." Examples include the upright rolling penny and a 3R planar robot arm with a passive first joint (actuator configuration $(0, 1, 1)$).
(ii) A 3R planar robot arm with a passive third joint (actuator configuration $(1, 1, 0)$), and with a passive second joint (actuator configuration $(1, 0, 1)$). The $(1, 1, 0)$ configuration was the original motivating example in [7], [8]. We present all the 3R planar robot configurations in Section IV-A.
(iii) Numerous vehicle models including the idealized planar hovercraft (planar body with two forces away from center of mass) and a rigid body in $SE(3)$ with three thrusters away from the center of mass. The dynamics of these systems are independent of the configuration, allowing simplified tests for decoupling vector fields. We present these systems in Section IV-B.

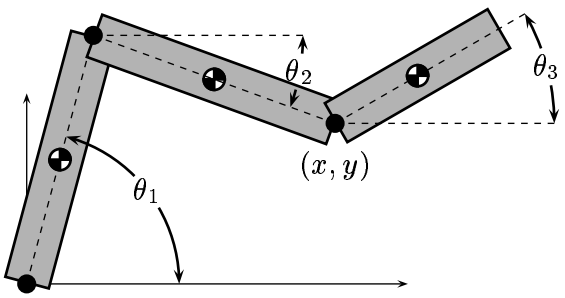

Fig. 1. Three-link 3R planar robot manipulator. This configuration is known as SCARA. The angles $(\theta_1, \theta_2, \theta_3)$ are measured counterclockwise. (x, y) is the location of the third joint.

A. Three link planar robot manipulator with a passive joint

We consider a three joint robot manipulator moving in a horizontal plane (see Figure 1). Different coordinates will be suited to different tasks: the set $(\theta_1, \theta_2, \theta_3)$ consists of the absolute angles (measured counterclockwise) of the three links with respect to the horizontal axis, the set (θ_1, r_2, r_3) measures the relative angles at the second and third joint, and (x, y, θ_3) measures the absolute location of the third joint and the absolute angle of the third link.

Three control actuator configurations are interesting depending on which control torque is missing. We do not consider settings in which two control torques are missing, since the resulting system is necessarily not kinematically controllable. For each of the interesting configurations, we present two decoupling vector fields such that their involutive closure is full rank. We therefore prove that each of the three configurations is kinematically controllable.

The computations that verify our statements are straightforward, although tedious. We refer to Appendix B for a careful implementation in Mathematica$^{\text{TM}}$. For reasons of brevity, we do not analyze the singularities of the decoupling vector fields and of their involutive closure.

Actuator configuration (0,1,1)

We rely on the coordinate system (θ_1, r_2, r_3). Accordingly, the input co-vector fields F_1, F_2, and the annihilator vector field X are

$$F_1 = dr_2, \;\; F_2 = dr_3, \;\; X = \frac{\partial}{\partial \theta_1}.$$

It is a straightforward computation to see that the inertia matrix M has the following structure:

$$\begin{bmatrix} M_{11}(r_2, r_3) & M_{12}(r_2, r_3) & M_{13}(r_2, r_3) \\ M_{12}(r_2, r_3) & M_{22}(r_3) & M_{23}(r_3) \\ M_{13}(r_2, r_3) & M_{23}(r_3) & M_{33} \end{bmatrix}. \qquad (14)$$

In other words, the components of the inertia matrix are independent of θ_1 and depend on (r_2, r_3) in a specific manner. We refer to Appendix A for the expressions for the inertia's entries.

The system is locally kinematically controllable and two decoupling vector fields are

$$\begin{aligned} V_1 &= (M_{13}M_{23} - M_{33}M_{12})\frac{\partial}{\partial \theta_1} + (M_{33}M_{11} - M_{13}^2)\frac{\partial}{\partial r_2} \\ &\quad + (M_{12}M_{13} - M_{11}M_{23})\frac{\partial}{\partial r_3}, \\ V_2 &= (M_{12}M_{23} - M_{13}M_{22})\frac{\partial}{\partial \theta_1} + (M_{12}M_{13} - M_{11}M_{23})\frac{\partial}{\partial r_2} \\ &\quad + (M_{11}M_{22} - M_{12}^2)\frac{\partial}{\partial r_3}. \end{aligned}$$

Note that V_1 and V_2 are scalar multiples of $Y_1 = M^{-1}F_1$, and $Y_2 = M^{-1}F_2$.

Remark IV.1 (Designing the decoupling vector fields) The key observation is that the system has a *symmetry* [23] and a conserved quantity, that is, angular momentum about the first joint. A non-trivial consequence of the conservation law is that $\langle\langle \nabla_{V_i} V_j \, , \, X \rangle\rangle = 0$ for $i, j \in \{1, 2\}$. Accordingly, one can prove not only that the system is locally kinematically controllable, but also that it is indeed kinematic, as defined in [27].

Actuator configuration (1,0,1)

Since this configuration resembles the $(0, 1, 1)$ setting, we rely on the same coordinate system and on the expression for the inertia matrix M given in equation (14). The input co-vector fields F_1, F_2, and the annihilator vector field X are

$$F_1 = d\theta_1, \;\; F_2 = dr_3, \;\; X = \frac{\partial}{\partial r_2}.$$

The system is locally kinematically controllable and two decoupling vector fields are

$$\begin{aligned} V_1 &= -M_{23}\frac{\partial}{\partial r_2} + M_{22}\frac{\partial}{\partial r_3} \\ V_2 &= 2\left(M_{23}\frac{\partial M_{12}}{\partial r_2} - M_{22}\frac{\partial M_{13}}{\partial r_2}\right)\frac{\partial}{\partial \theta_1} \\ &\quad + \left(2M_{12}\frac{\partial M_{13}}{\partial r_2} - M_{23}\frac{\partial M_{11}}{\partial r_2}\right)\frac{\partial}{\partial r_2} \\ &\quad + \left(M_{22}\frac{\partial M_{11}}{\partial r_2} - 2M_{12}\frac{\partial M_{12}}{\partial r_2}\right)\frac{\partial}{\partial r_3}. \end{aligned}$$

Remark IV.2 (Designing the decoupling vector fields) At fixed angle θ_1, the system has a symmetry about the angle r_2. The first vector field is designed as discussed in the previous remark. The second vector field is identified solving a quadratic equation of the form (13).

Actuator configuration (1,1,0)

We rely on the coordinate system (x, y, θ_3). The kinetic energy of the first two links can be written as

$$\frac{1}{2}\begin{bmatrix} \dot{x} \\ \dot{y} \end{bmatrix}^T \begin{bmatrix} M_{11}(x, y) & M_{12}(x, y) \\ M_{12}(x, y) & M_{22}(x, y) \end{bmatrix} \begin{bmatrix} \dot{x} \\ \dot{y} \end{bmatrix}. \qquad (15)$$

Let m_3, I_3 denote the mass and moment of inertia of the third link; let l_3 be the distance from the third joint to the center of mass of the third link. The kinetic energy of the third link is

$$\begin{aligned} &\frac{1}{2}(I_3 + m_3 l_3^2)\dot{\theta}_3^2 + \frac{1}{2}m_3(\dot{x}^2 + \dot{y}^2) \\ &\qquad + m_3 l_3 \dot{\theta}_3(\dot{y}\cos\theta_3 - \dot{x}\sin\theta_3). \end{aligned}$$

The input co-vector fields F_1, F_2, and the annihilator vector field X can be written as

$$F_1 = dx, \;\; F_2 = dy, \;\; X = \frac{\partial}{\partial \theta_3}.$$

The system is locally kinematically controllable, and two decoupling vector fields are

$$\begin{aligned} V_1 &= \cos\theta_3 \frac{\partial}{\partial x} + \sin\theta_3 \frac{\partial}{\partial y} \\ V_2 &= \sin\theta_3 \frac{\partial}{\partial x} - \cos\theta_3 \frac{\partial}{\partial y} + \frac{1}{\lambda}\frac{\partial}{\partial \theta_3}, \end{aligned}$$

where $\lambda = (I_3 + m_3 l_3^2)/m_3 l_3$. These motions are translation along the third link and rotation of the third link about its center of percussion, respectively.

Remark IV.3 (Designing the decoupling vector fields) A discussion on the design of these vector fields is presented in [7], [8]. The key observation is that the system has analog properties of that of a planar body endowed with two control forces acting on a point distant from the center of mass.

B. Vehicles with symmetry

If the inertia matrix of the mechanical system is independent of the system's configuration, the various quantities and operations involved in the definition of decoupling vector fields simplify considerably. This happens for example in a class of vehicle models whose kinetic energy is invariant under displacement (translations and rotations). While the coordinate-free formalism in Section II applies to this setting, there is enough additional structure to this class of systems to warrant a special treatment.

An *(left) invariant system on a Lie group* is a mechanical control system as defined in Section II where
(i) the configuration space is a Lie group G, and the linear space of body-fixed velocities is the Lie algebra $\mathfrak{g}$ of G; we let $g \in G$ denote the configuration of the system, and $\xi \in \mathfrak{g}$ denote the body-fixed velocity. Furthermore, we let $[\xi, \eta]$ denote the Lie bracket operation on $\mathfrak{g}$, and, given $\xi \in \mathfrak{g}$ we define its adjoint operator $\mathrm{ad}_\xi : \mathfrak{g} \to \mathfrak{g}$ as $\mathrm{ad}_\xi \, \eta = [\xi, \eta]$,
(ii) the kinetic energy of the system is invariant under displacements, and can be written in the form $\frac{1}{2}\xi^T \mathbb{I} \xi$, where the inertia matrix $\mathbb{I}$ is a positive-definite tensor over $\mathfrak{g}$, and
(iii) $\{F_a \in \mathfrak{g}^* : a = 1, \ldots, m\}$ are body-fixed forces, that is, input co-vectors, and $\{Y_a = \mathbb{I}^{-1} F_a \in \mathfrak{g} : a = 1, \ldots, m\}$ are input vectors.
The Lie group G is usually the matrix group of rigid displacements $SE(3)$, one of its subgroups, or multiple copies of one of its subgroups. For example, a satellite's attitude belongs to the group of special orthogonal matrices $SO(3)$. Over these matrix Lie groups, the operation of Lie bracket can be performed without differentiation, and is equivalent to the matrix commutator. We refer to [24] for more details on the group $SE(3)$ and its algebra $\mathfrak{se}(3)$.

The equations of motion (3) written in terms of the body-fixed velocity ξ reduce to

$$\dot{\xi} = \mathbb{I}^{-1} \, \mathrm{ad}_\xi^T \, \mathbb{I} \xi + \sum_{a=1}^{m} Y_a u_a(t). \tag{16}$$

These equations are referred to as the Euler-Poincaré equations; see [23], [24], [21]. Consider the $(m < n)$-dimensional subspace generated by the input co-vectors $\mathrm{span}\{F_1, \ldots, F_m\}$. Its annihilator is an $(n - m)$-dimensional subspace generated by vectors $\{X_1, \ldots, X_{n-m}\}$, such that

$$F_a{}^T X_c = 0$$

for all $1 \le a \le m, 1 \le c \le n - m$. A curve $g : [0, T] \mapsto G$ is a solution to the underactuated system in equation (16) if and only if it satisfies the $n - m$ constraints

$$0 = X_c{}^T \sum_{a=1}^{m} u_a F_a = X_c{}^T \left(\mathbb{I} \dot{\xi} - \mathrm{ad}_\xi^T \, \mathbb{I} \xi \right).$$

Next, we revisit the treatment in Lemma III.2 on decoupling vectors and kinematic controllability. A vector $V \in \mathfrak{g}$ is decoupling if and only if it satisfies

$$V^T \mathbb{I} \, X_c = 0 \tag{17}$$

$$\left(\mathbb{I}^{-1} \, \mathrm{ad}_V^T \, \mathbb{I} V \right)^T \mathbb{I} X_c = V^T \mathbb{I} \, [V, X_c] = 0, \tag{18}$$

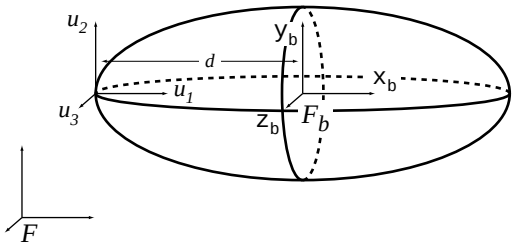

Fig. 2. A rigid body with three thrusters.

for all $c = 1, \ldots, n - m$. Note that equations (17), (18) do not depend on g and require no symbolic differentiation.

Finally, we revisit the discussion in Section III-A on computing decoupling vectors fields. Any decoupling vector field is written as a linear combination of the input vectors

$$V = \sum_{a=1}^{m} h^a Y_a,$$

where $h^1, \ldots, h^m$ are scalar constants. Define the $(n - m)$ matrices $B^c \in \mathbb{R}^{m \times m}$ according to

$$B^c_{a,b} = Y_a^T \mathbb{I} \, \mathrm{ad}_{Y_b} \, X_c.$$

Mimicking the treatment leading to equation (13), we let $h = [h^1, \ldots, h^m]^T \in \mathbb{R}^m$ and simplify the condition in equation (17) to

$$h^T B^c h = 0 \tag{19}$$

for all $c = 1, \ldots, n - m$. If h is a solution to these $(n - m)$ quadratic constraints, then so is αh for all $\alpha \in \mathbb{R}$, and in particular $\alpha = 0$. To disregard this trivial solution, we can impose the additional quadratic constraint $h^T h = 1$. In summary, decoupling vector fields are computed by solving $(n - m + 1)$ quadratic equations in h. Any solution to these equations defines a decoupling vector field $V = \sum_a h^a Y_a$.

B.1 A three-dimensional underwater vehicle

We consider the case of a neutrally buoyant underwater vehicle moving in ideal fluid. Recall that the motion of a rigid body in incompressible, irrotational and inviscid fluid is Hamiltonian with an inertia tensor which includes added masses and inertias; see [28], [21]. The case of a vehicle moving in space (no gravity and no aerodynamic forces) is obtained by setting the added masses to zero.

A frame $\mathcal{F}_b$ is attached to the center of mass of the body and aligned with the principal axes of inertia (see Figure 2). The configuration of the body is the matrix $g \in SE(3)$ representing the displacement of $\mathcal{F}_b$ relative to an inertial frame $\mathcal{F}$. We write

$$g = \begin{bmatrix} R & p \\ 0 & 1 \end{bmatrix},$$

or simply $g = (R, p)$ for shorthand, where $R \in SO(3)$ is a 3×3 rotation matrix and $p \in \mathbb{R}^3$ is the position of the origin of $\mathcal{F}_b$ in $\mathcal{F}$. The velocity of the rigid body is an element ξ of $\mathfrak{se}(3) = \mathbb{R}^6$, the Lie algebra associated to $SE(3)$. We

write $\xi = (\omega, v)$, where $\omega \in \mathbb{R}^3$ is the angular velocity and $v \in \mathbb{R}^3$ is the linear velocity of the body written in $\mathcal{F}_b$. The kinematic equations are

$$\dot{R} = R\widehat{\omega}, \qquad \dot{p} = Rv,$$

where the map $\widehat{\cdot}$ gives the 3×3 skew-symmetric matrix representation of a vector in $\mathbb{R}^3$, that is, in coordinates

$$\widehat{\begin{bmatrix} a_1 \\ a_2 \\ a_3 \end{bmatrix}} = \begin{bmatrix} 0 & -a_3 & a_2 \\ a_3 & 0 & -a_1 \\ -a_2 & a_1 & 0 \end{bmatrix}.$$

To write the equations of motion as in equation (16), we need to introduce the ad operator and the inertia matrix. As shown in [24], one computes

$$\mathrm{ad}_\xi = \mathrm{ad}_{(\omega,v)} = \begin{bmatrix} \widehat{\omega} & 0 \\ \widehat{v} & \widehat{\omega} \end{bmatrix}.$$

The kinetic energy of the vehicle is written

$$\frac{1}{2}\xi^T \mathbb{I} \xi = \frac{1}{2}\omega^T \mathbb{J} \omega + \frac{1}{2} v^T \mathbb{M} v,$$

where the inertia matrix $\mathbb{I}$ is block-diagonal with components $\mathbb{J}$ and $\mathbb{M}$, and where $\mathbb{M} = \mathrm{diag}\{m_{\mathtt{x_b}}, m_{\mathtt{y_b}}, m_{\mathtt{z_b}}\}$ and $\mathbb{J} = \mathrm{diag}\{J_{\mathtt{x_b}}, J_{\mathtt{y_b}}, J_{\mathtt{z_b}}\}$ include any added masses. The dynamic equations (with no external forces) are

$$\begin{aligned} \mathbb{J}\dot{\omega} &= \mathbb{J}\omega \times \omega + \mathbb{M} v \times v \\ \mathbb{M}\dot{v} &= \mathbb{M} v \times \omega. \end{aligned}$$

Next we present the external forces. The case of a vehicle subject to a force through the center of mass and three independent torques is a direct generalization of the planar body with a pure force and torque; see Section III. Instead, assume the body is endowed with three body-fixed control forces applied at a point a distance d from the center of mass (see Figure 2). In other words, the three control forces u_1, u_2, u_3 act along lines parallel to the $\mathtt{x_b}, \mathtt{y_b}, \mathtt{z_b}$ axes, respectively, at a point $(-d, 0, 0)$, $d > 0$ in $\mathcal{F}_b$. The corresponding input vectors are

$$Y_1 = \frac{1}{m_{\mathtt{x_b}}} \begin{bmatrix} 0 \\ 0 \\ 0 \\ 1 \\ 0 \\ 0 \end{bmatrix}, \quad Y_2 = -\frac{d}{J_{\mathtt{z_b}}} \begin{bmatrix} 0 \\ 0 \\ 1 \\ 0 \\ 0 \\ 0 \end{bmatrix} + \frac{1}{m_{\mathtt{y_b}}} \begin{bmatrix} 0 \\ 0 \\ 0 \\ 0 \\ 1 \\ 0 \end{bmatrix},$$

$$Y_3 = \frac{d}{J_{\mathtt{y_b}}} \begin{bmatrix} 0 \\ 1 \\ 0 \\ 0 \\ 0 \\ 0 \end{bmatrix} + \frac{1}{m_{\mathtt{z_b}}} \begin{bmatrix} 0 \\ 0 \\ 0 \\ 0 \\ 0 \\ 1 \end{bmatrix},$$

and the constraint subspace is generated by

$$X_1 = \begin{bmatrix} 1 \\ 0 \\ 0 \\ 0 \\ 0 \\ 0 \end{bmatrix}, \quad X_2 = \begin{bmatrix} 0 \\ 0 \\ 1 \\ 0 \\ 0 \\ 0 \end{bmatrix} + d \begin{bmatrix} 0 \\ 0 \\ 0 \\ 0 \\ 1 \\ 0 \end{bmatrix}, \quad X_3 = \begin{bmatrix} 0 \\ 1 \\ 0 \\ 0 \\ 0 \\ 0 \end{bmatrix} - d \begin{bmatrix} 0 \\ 0 \\ 0 \\ 0 \\ 0 \\ 1 \end{bmatrix}.$$

Decoupling motions for this system are found by solving the quadratic equations (19). A direct computation shows that

$$Y_a^T \mathbb{I}\, \mathrm{ad}_{Y_a} X_c = 0$$

for all $a = 1, 2, 3$, and $c = 1, 2, 3$, so that the vectors Y_1, Y_2, Y_3 are easily shown to be decoupling. The Lie bracket analysis is also relatively straightforward: Y_1 corresponds to a translation along the body axis $\mathtt{x_b}$, Y_3 corresponds to a translation along $\mathtt{z_b}$ and a rotation about $\mathtt{y_b}$, and a similar statement holds for Y_2. A simple calculation shows that $[Y_1, Y_3]$ is a translation along $\mathtt{y_b}$ and $[Y_1, Y_2]$ is a translation along $\mathtt{z_b}$. The Lie bracket $[Y_2, Y_3]$ is the sum of three terms, one of which is rotation about $\mathtt{x_b}$. The six vectors $\{Y_1, Y_2, Y_3, [Y_1, Y_3], [Y_1, Y_2], [Y_2, Y_3]\}$ are therefore linearly independent, and the vehicle is locally kinematically controllable.

V. Trajectory Planning

Trajectory planning between zero velocity states can be decoupled into path planning on the configuration space using the decoupling velocities $V_1, \ldots, V_p$, followed by time scaling of the path according to actuator limits. This decoupling halves the dimension of the search space, reducing the computational complexity of the motion planner. However, the decoupling also precludes the possibility of finding globally time-optimal trajectories, since the path planner has no notion of actuator limits. Instead, we search for sub-time-optimal motion plans by asking the path planner to minimize the number of switches between decoupling vector fields. This minimizes the number of times the system velocity must be brought to zero, resulting in fast motions in practice.

A decoupled trajectory planner for the 3R robot arm with a passive third joint was presented in [7], [8]. This planner takes into account obstacles, workspace limits, and joint limits. Future work will address collision-free path planning minimizing the number of switches for more general kinematically controllable systems.

A. Trajectory planning via inverse kinematics

Here we briefly consider the problem of trajectory planning without obstacles for a locally kinematically controllable three-dimensional body from an initial g_0 to a final displacement g_f belonging to $SE(3)$. Since $SE(3)$ is six-dimensional, any arbitrary motion requires generically six motion segments and five switches between decoupling motions. Each segment follows the flow of a left-invariant decoupling vector field V_i, $i \in \{1, \ldots, p\}$. Using the matrix exponential notation $e : se(3) \to SE(3)$, the path planning problem is to solve the inverse kinematics problem

$$g_f = g_0 e^{r_1 V_{i_1}} e^{r_2 V_{i_2}} e^{r_3 V_{i_3}} e^{r_4 V_{i_4}} e^{r_5 V_{i_5}} e^{r_6 V_{i_6}}$$

for $r_1, \ldots, r_6 \in \mathbb{R}$, and $i_1, \ldots i_6 \in \{1, \ldots, p\}$. We refer to [24, Chapter 3] for a treatment on inverse kinematics.

As an example, consider a spacecraft with three thrusters, as in Figure 2. The mass matrix of the spacecraft is $\mathbb{M} = \mathrm{diag}\{m, m, m\}$ and its inertia matrix is

$\mathbb{J} = \text{diag}\{J_{\mathtt{x_b}}, J_{\mathtt{y_b}}, J_{\mathtt{z_b}}\}$. By the analysis of Section IV-B.1, this spacecraft is locally kinematically controllable. By analogy to the 3R manipulator with a passive third joint in Section IV-A, decoupling motions for this vehicle are translation along the body $\mathtt{x_b}$-axis (V_1), rotation about the center of percussion in the $\mathtt{x_b} - \mathtt{y_b}$ plane (V_2), and rotation about the center of percussion in the $\mathtt{x_b} - \mathtt{z_b}$ plane (V_3). If the thrusters are located at $(-d, 0, 0)$ in $\mathcal{F}_b$ and $J_{\mathtt{y_b}} = J_{\mathtt{z_b}}$, then the centers of percussion in the $\mathtt{x_b} - \mathtt{y_b}$ and $\mathtt{x_b} - \mathtt{z_b}$ planes are coincident at $\mathtt{CP} = (J_{\mathtt{y_b}}/(md), 0, 0)$. For simplicity, we make this assumption.

The configuration of the spacecraft is represented by the body-fixed frame $\mathcal{F}_p$, which is aligned with $\mathcal{F}_b$ and located at $\mathtt{CP}$. The axes of $\mathcal{F}_p$ are written $\{\mathtt{x_p}, \mathtt{y_p}, \mathtt{z_p}\}$. Define $\mathcal{F}_0$ to be coincident with $\mathcal{F}_p$ when the spacecraft is at its initial configuration. Without loss of generality, let $\mathcal{F}_0$ be coincident with $\mathcal{F}$, and call this configuration $g_0 = (I, 0)$, where I is the 3×3 identity matrix. g_f is defined by the frame $\mathcal{F}_g$, coincident with $\mathcal{F}_p$ at the goal configuration. The origin of $\mathcal{F}_g$ is located at (x_g, y_g, z_g) in $\mathcal{F}$, and the axes of $\mathcal{F}_g$ are expressed in $\mathcal{F}$ as $\{\mathtt{x_g}, \mathtt{y_g}, \mathtt{z_g}\}$. The reconfiguration of the spacecraft can be accomplished by the following six-step sequence of decoupling motions, based on ZYZ Euler angles:

1: Rotate $\tan^{-1}(y_g, x_g)$ about $\mathtt{z_p}$. (This is the two-argument arctangent.)
2: Rotate $\tan^{-1}(z_g/\sqrt{x_g^2 + y_g^2})$ about $\mathtt{y_p}$. The $\mathtt{x_p}$-axis is now pointed toward the origin of $\mathcal{F}_g$.
3: Translate $\sqrt{x_g^2 + y_g^2 + z_g^2}$ along $\mathtt{x_p}$.
4: Rotate about $\mathtt{z_p}$ until $\mathtt{y_p}$ is perpendicular to $\mathtt{y_g}$.
5: Rotate about $\mathtt{y_p}$ until $\mathtt{z_p} = \mathtt{z_g}$.
6: Rotate about $\mathtt{z_p}$ until $\mathtt{y_p} = \mathtt{y_g}$.

Figure 3 shows an example path generated by this sequence. The spacecraft is a uniform density ellipsoid of length 2m in the $\mathtt{x_b}$ direction and diameter 1m in the $\mathtt{y_b} - \mathtt{z_b}$ plane. The mass of the spacecraft is 100kg, $J_{\mathtt{y_b}} = J_{\mathtt{z_b}} = 25\text{kg-m}^2$, and the two thrusters in the $\mathtt{y_b} - \mathtt{z_b}$ plane are located at $(-0.125\text{m}, 0, 0)$, yielding $\mathtt{CP} = (2\text{m}, 0, 0)$ in $\mathcal{F}_b$. The goal configuration of the spacecraft is

$$g_f = \begin{bmatrix} R_f & p_f \\ 0 & 1 \end{bmatrix} = \begin{bmatrix} 0 & 0 & 1 & 3\text{m} \\ 1 & 0 & 0 & 3\text{m} \\ 0 & 1 & 0 & 3\text{m} \\ 0 & 0 & 0 & 1 \end{bmatrix}.$$

Figure 4 shows the time-optimal thrust values if each thruster saturates at 100N. One thruster is always saturated. During translation, only thruster u_1 is activated, and the time-optimal thrust is bang-bang. During rotation, u_1 is proportional to the square of the angular velocity, to keep the rotation axis fixed. The bounds on u_1 define a maximum angular velocity. In this example, this maximum angular velocity is attained during the final two rotations, implying that u_1 is saturated and the thruster providing torque must be shut off until it is time to slow the motion. In this example, the entire motion is completed in 19.16 seconds.

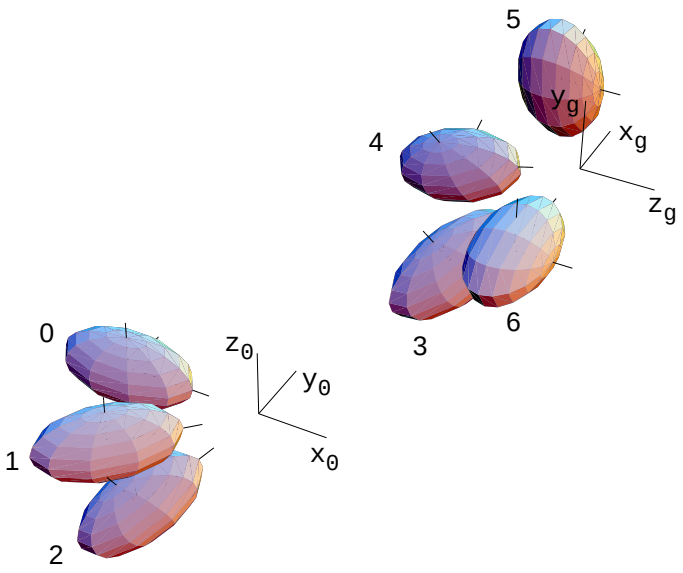

Fig. 3. A six-step sequence to reconfigure the spacecraft with three thrusters. The initial and final configuration of the center of percussion frame is shown. The location of the thrusters is chosen to put the center of percussion outside the body to make the rotational motions easier to see.

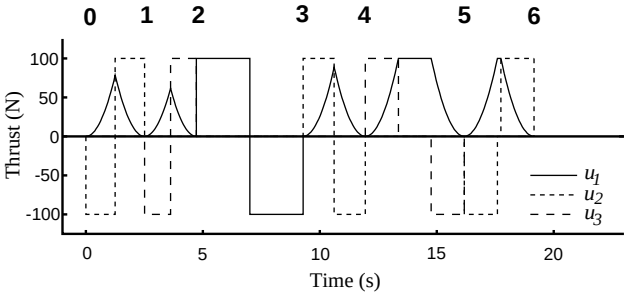

Fig. 4. The time-optimal thruster actuations for the spacecraft path in Figure 3. The corresponding stages of the motion are shown above the plot.

VI. Conclusion

The notions of decoupling vector fields and kinematic controllability allow us to use the structure of underactuated mechanical systems to reduce the computational complexity of collision-free trajectory planning. While a kinematic path planners already exist for some kinematically controllable systems (see, e.g., [7], [8]), future work will be toward constructing a path planner for general locally kinematically controllable systems. Trajectories found by the decoupled approach can be further locally optimized to smooth out transitions between decoupling vector fields (eliminating stops) while still satisfying the underactuation constraints, resulting in faster motions. For robust execution of the planned trajectories, we plan to study feedback stabilization of kinematic motions.

Acknowledgments

We thank the reviewers for their many comments on improving the exposition. This work was funded by the Cam-

pus Research Board of the University of Illinois and NSF grant IIS-9811571.

References

[1] J. E. Bobrow, S. Dubowsky, and J. S. Gibson, "Time-optimal control of robotic manipulators along specified paths," *International Journal of Robotics Research*, vol. 4, no. 3, pp. 3–17, 1985.

[2] K. G. Shin and N. D. McKay, "Minimum-time control of robotic manipulators with geometric path constraints," *IEEE Transactions on Automatic Control*, vol. 30, no. 6, pp. 531–541, 1985.

[3] F. Pfeiffer and R. Johanni, "A concept for manipulator trajectory planning," *IEEE Journal of Robotics and Automation*, vol. 3, no. 2, pp. 115–123, 1987.

[4] J.-J. E. Slotine and H. S. Yang, "Improving the efficiency of time-optimal path-following algorithms," *IEEE Transactions on Robotics and Automation*, vol. 5, no. 1, pp. 118–124, 1989.

[5] Z. Shiller and H.-H. Lu, "Computation of path constrained time optimal motions with dynamic singularities," *ASME Journal on Dynamic Systems, Measurement, and Control*, vol. 114, pp. 34–40, 1992.

[6] Z. Shiller and S. Dubowsky, "On computing the global time-optimal motions of robotic manipulators in the presence of obstacles," *IEEE Transactions on Robotics and Automation*, vol. 7, no. 6, pp. 785–797, 1991.

[7] K. M. Lynch, N. Shiroma, H. Arai, and K. Tanie, "Collision-free trajectory planning for a 3-DOF robot with a passive joint," *International Journal of Robotics Research*, vol. 19, no. 12, pp. 1171–1184, 2000.

[8] K. M. Lynch, N. Shiroma, H. Arai, and K. Tanie, "Motion planning for a 3-DOF robot with a passive joint," in *IEEE Int. Conf. on Robotics and Automation*, (Leuven, Belgium), pp. 927–32, May 1998.

[9] J. Barraquand and J.-C. Latombe, "Nonholonomic multibody mobile robots: Controllability and motion planning in the presence of obstacles," *Algorithmica*, vol. 10, no. 2-3-4, pp. 121–155, 1993.

[10] J.-P. Laumond, P. Jacobs, M. Taix, and R. M. Murray, "A motion planner for nonholonomic mobile robots," *IEEE Transactions on Robotics and Automation*, vol. 10, no. 5, pp. 577–593, 1994.

[11] C. O'Dunlaing, "Motion planning with inertial constraints," *Algorithmica*, vol. 2, no. 4, pp. 431–475, 1987.

[12] J. Canny, A. Rege, and J. Reif, "An exact algorithm for kinodynamic planning in the plane," *Discrete and Computational Geometry*, vol. 6, pp. 461–484, 1991.

[13] B. Donald, P. Xavier, J. Canny, and J. Reif, "Kinodynamic motion planning," *Journal of the Association for Computing Machinery*, vol. 40, no. 5, pp. 1048–66, 1993.

[14] B. Donald and P. Xavier, "Provably good approximation algorithms for optimal kinodynamic planning: Robots with decoupled dynamics bounds," *Algorithmica*, vol. 14, no. 6, pp. 443–479, 1995.

[15] B. Donald and P. Xavier, "Provably good approximation algorithms for optimal kinodynamic planning for Cartesian robots and open chain manipulators," *Algorithmica*, vol. 14, no. 6, pp. 480–530, 1995.

[16] J. Reif and H. Wang, "Non-uniform discretization approximations for kinodynamic motion planning," in *Algorithms for Robotic Motion and Manipulation* (J.-P. Laumond and M. Overmars, eds.), pp. 97–112, Boston, MA: A. K. Peters, 1997.

[17] S. M. LaValle and J. J. Kuffner, "Randomized kinodynamic planning," in *IEEE Int. Conf. on Robotics and Automation*, (Detroit, MI), pp. 473–479, May 1999.

[18] S. M. LaValle and J. J. Kuffner, "Rapidly-exploring random trees: Progress and prospects," in *Workshop on Algorithmic Foundations of Robotics*, (Dartmouth, NH), Mar. 2000.

[19] D. Hsu, R. Kindel, J.-C. Latombe, and S. Rock, "Randomized kinodynamic motion planning," in *Workshop on Algorithmic Foundations of Robotics*, (Dartmouth, NH), p. ?, Mar. 2000.

[20] A. D. Lewis and R. M. Murray, "Configuration controllability of simple mechanical control systems," *SIAM Journal on Control and Optimization*, vol. 35, no. 3, pp. 766–790, 1997.

[21] F. Bullo, N. E. Leonard, and A. D. Lewis, "Controllability and motion algorithms for underactuated Lagrangian systems on Lie groups," *IEEE Transactions on Automatic Control*, vol. 45, no. 8, pp. 1437–1454, 2000.

[22] M. P. Do Carmo, *Riemannian Geometry*. Boston, MA: Birkhäuser, 1992.

[23] J. E. Marsden and T. S. Ratiu, *Introduction to Mechanics and Symmetry*. New York, NY: Springer Verlag, second ed., 1999.

[24] R. M. Murray, Z. X. Li, and S. S. Sastry, *A Mathematical Introduction to Robotic Manipulation*. Boca Raton, FL: CRC Press, 1994.

[25] H. J. Sussmann, "A general theorem on local controllability," *SIAM Journal on Control and Optimization*, vol. 25, no. 1, pp. 158–194, 1987.

[26] S. D. Kelly and R. M. Murray, "Geometric phases and robotic locomotion," *Journal of Robotic Systems*, vol. 12, no. 6, pp. 417–431, 1995.

[27] A. D. Lewis, "When is a mechanical control system kinematic?," in *IEEE Conf. on Decision and Control*, (Phoenix, AZ), pp. 1162–1167, Dec. 1999.

[28] H. Lamb, *Hydrodynamics*. New York, NY: Dover Publications, sixth ed., 1932.

Appendix

I. Inertia matrices for planar three-link manipulator

For completeness, we report the explicit expression of the inertia matrix as in equation (14). The expression for the inertia in the (x, y, θ_3) coordinate system is too onerous to report here.

$$
\begin{aligned}
M_{11}(r_2, r_3) &= I_1 + I_2 + I_3 + l_1^2 m_1/4 + l_1^2(m_2 + m_3) + l_2^2 m_3 \\
&\quad + (l_3^2 m_3 + l_2^2 m_2)/4 + l_1 l_2 (m_2 + 2m_3)\cos(r_2) \\
&\quad + l_2 l_3 m_3 \cos(r_3) + l_1 l_3 m_3 \cos(r_2 + r_3) \\
M_{12}(r_2, r_3) &= I_2 + I_3 + l_2^2(m_2/4 + m_3) + l_3^2 m_3/4 \\
&\quad + l_1 l_2 (m_2 + 2m_3)\cos(r_2)/2 + l_2 l_3 m_3 \cos(r_3) \\
&\quad + l_1 l_3 m_3 \cos(r_2 + r_3)/2 \\
M_{13}(r_2, r_3) &= I_3 + l_3^2 m_3/4 + l_2 l_3 m_3 \cos(r_3)/2 \\
&\quad + l_1 l_3 m_3 \cos(r_2 + r_3)/2 \\
M_{22}(r_3) &= I_2 + I_3 + l_2^2(m_2/4 + m_3) + l_3^2 m_3/4 \\
&\quad + l_2 l_3 m_3 \cos(r_3) \\
M_{23}(r_3) &= I_3 + l_3^2 m_3/4 + l_2 l_3 m_3 \cos(r_3)/2 \\
M_{33} &= I_3 + l_3^2 m_3/4.
\end{aligned}
$$

II. Symbolic computations

It is important to emphasize the difficulty of the symbolic computations defined in the theoretical developments on modeling and kinematic controllability. While the mathematical definitions are straightforward, only a careful implementation leads to a speedy execution on a modern workstation. In the Mathematica™ code below, we employ two main arrangements to maximize efficiency: we select appropriate coordinate systems for each setting, and we emphasize functional dependencies instead of substituting the exact values of M.

We start by presenting the code to compute the Levi-Civita connection of a mechanical system (i.e., its Christoffel symbols as in equation (4)), and the covariant derivative of vector fields (equation (6)).

```
BeginPackage["MechSys`"]

LeviCivita::usage = "LeviCivita[M,x] computes
  the Christoffel symbols of the Levi-Civita
  connection for the mechanical system with inertia
```

```
  matrix M with respect to the coordinates x.";
CovariantDer::usage = "CovariantDer[X,Y,Nabla,x]
  computes the covariant derivative of Y along X
  with respect to a connection Nabla in coordinates x.";

Begin["Private`"]
LeviCivita[M_, x_] :=
    Module[{Minv=Inverse[M],i,j,k,h,N=Length[x]},
    Table[ Sum[ Minv[[h,k]] ( D[M[[h,j]], x[[i]]] +
    D[M[[i,h]], x[[j]]] - D[M[[i,j]], x[[h]]] ) / 2,
    {h,N}], {k,N}, {j,N}, {i,N} ]];
CovariantDer[X_, Y_, Nabla_, x_] :=
    Module[{i,j,k,N=Length[x]},
    Table[ Sum[ D[Y[[i]],x[[j]]] X[[j]] +
    Sum[ Nabla[[i,j,k]] X[[j]] Y[[k]],
    {k,N}], {j,N}], {i,N} ]];
End[] EndPackage[]
```

Next, we present the code to study the three actuator configurations in the three link planar robot manipulator. We treat the $(0,1,1)$ and $(1,0,1)$ systems jointly as they rely on the same coordinate system. The inertia matrix is as in equation (14).

```
(** Mathematica code for SCARA 011 & 101   **
 ** Configuration, inertia, and connection **)
Needs["MechSys`"];
q = {th1,r2,r3};
M = {{M11[r2,r3],  M12[r2,r3],  M13[r2,r3]},
     {M12[r2,r3],  M22[r3],     M23[r3]   },
     {M13[r2,r3],  M23[r3],     M33       }};
nabla = LeviCivita[M, q];

(** SCARA 011 : decoupling vector fields and **
 ** their covariant derivatives              **)
V1 = {M[[1,3]]M[[2,3]] - M[[3,3]]M[[1,2]],
      M[[3,3]]M[[1,1]] - M[[1,3]]^2,
      M[[1,2]]M[[1,3]] - M[[1,1]]M[[2,3]]};
V2 = {M[[1,2]]M[[2,3]] - M[[1,3]]M[[2,2]],
      M[[1,2]]M[[1,3]] - M[[1,1]]M[[2,3]],
      M[[1,1]]M[[2,2]] - M[[1,2]]^2};
V11 = CovariantDer[V1, V1, nabla, q];
V22 = CovariantDer[V2, V2, nabla, q];

(** Control annihilator, and vanishing quantities **)
X = {1,0,0}; Simplify[{V1.M.X, V11.M.X, V2.M.X, V22.M.X}]

(** SCARA 101 : decoupling vector fields and **
 ** their covariant derivatives              **)
V1 = {0, -M[[2,3]], M[[2,2]]};
V2 = {2M[[2,3]] D[M[[1,2]],r2] - 2M[[2,2]] D[M[[1,3]],r2],
      2M[[1,2]] D[M[[1,3]],r2] - M[[2,3]] D[M[[1,1]],r2],
      M[[2,2]] D[M[[1,1]],r2] - 2M[[1,2]] D[M[[1,2]],r2]};
V11 = CovariantDer[V1, V1, nabla, q];
V22 = CovariantDer[V2, V2, nabla, q];

(** Control annihilator, and vanishing quantities **)
X = {0,1,0}; Simplify[{V1.M.X, V11.M.X, V2.M.X, V22.M.X}]
```

Finally, we present the $(1,1,0)$ case. The inertia matrix is as in equation (15). To streamline the computations, we redefine the terms $\{M_{11}, M_{12}, M_{22}\}$ to account for the term $\frac{1}{2}m_3(\dot{x}^2+\dot{y}^2)$, and we scale them by a factor $m_3 l_3$.

```
(** Mathematica code for SCARA 110.        **
 ** Configuration, inertia, and connection **)
Needs["MechSys`"];
q = {x,y,th3};
M = {{M11[x,y],    M12[x,y],  -Sin[th3]},
     {M12[x,y],    M22[x,y],  Cos[th3] },
     {-Sin[th3],   Cos[th3],  lambda   }};
nabla = Simplify[ LeviCivita[M, q]];

(** decoupling vector fields and **
 ** their covariant derivatives  **)
V1 = {Cos[th3], Sin[th3], 0};
V2 = {Sin[th3], -Cos[th3], 1/lambda };
V11 = CovariantDer[V1, V1, nabla, q];
V22 = CovariantDer[V2, V2, nabla, q];

(** Control annihilator, and vanishing quantities **)
X = {0,0,1}; Simplify[{V1.M.X, V11.M.X, V2.M.X, V22.M.X}]
```